

Failure analysis of hybrid sandwich structures with different cladding materials

Michał Rogala^{1*} , Roman Kaczyński², Jakub Gajewski¹, Katarzyna Gawdzińska³

¹ Faculty of Mechanical Engineering, Department of Machine Design & Mechatronics, Lublin University of Technology, ul. Nadbystrzycka 36, 20-618 Lublin, Poland

² Faculty of Mechanical Engineering, Białystok University of Technology, ul. Wiejska 45A, 15-351 Białystok, Poland

³ Faculty of Mechanical Engineering, Maritime University of Technology, ul. Willowa 2, 71-650 Szczecin, Poland

* Corresponding author's e-mail: m.rogala@pollub.pl

ABSTRACT

The dynamic development of the automotive and aviation industry has resulted in the continuous improvement of sandwich structures. These structures are lightweight and strong due to the application of lightweight materials as their core. The structure finds particular application in automotive or aerospace vehicles, which are focused on minimizing the weight of the structure, which translates into operating costs. The use of sandwich structures carries risks due to cladding debonding. The present study is intended to analyze the failure mechanism of structures based on aluminum foam with three types of cladding: aluminum sheet, carbon fiber plate and linen fiber plate. The structures were subjected to three-point bending during which the ability to transfer mechanical stress was observed, as well as the failure mechanism resulting from failure of the adhesive bond, core or cladding. Studies conducted revealed a significant contribution from the porous core. The tests showed similar load transfer and mechanical energy absorption capacities for the analyzed samples. The flax composite exhibited the lowest capacity, where destruction occurred from approximately 800 N for the analyzed sample geometry. Despite similar load-carrying capacity, different types of structural failure were recorded, such as delamination, cladding debonding and metal foam pore cracking detailed in the paper.

Keywords: sandwich structures, fiber composite, aluminum foam, porous structures, failure analysis.

INTRODUCTION

Nowadays, the design of engineering structures seeks to reduce the weight of components. Technological advances make it possible to manufacture thin components made of fiber composites. Sandwich structures, characterized by their unique configuration of a lightweight core material sandwiched between two outer layers, have garnered significant attention in various engineering applications due to their exceptional mechanical properties and energy absorption capabilities [1, 2]. Among these, aluminum foam has emerged as a popular core material owing to its lightweight nature, high specific strength, and remarkable energy-dissipation characteristics [3, 4]. Coupling

aluminum foam with composite cladding creates a hybrid structure that exploits the advantages of both materials, enhancing performance in structural applications such as aerospace, automotive, and civil engineering [5–7]. In the literature, numerous materials are utilized as fibers within an epoxy resin matrix. The most commonly employed fibers are glass or carbon; however, many publications describe the application of natural fibers, including flax, bamboo, or banana [8–10]. Depending on the type of reinforcement and matrix used, as well as the orientation of the fibers, it is possible to obtain a material with desired mechanical and material properties while maintaining a low mass of the element. Due to their modification potential, fiber composites have

found applications in various industrial sectors, including aviation, marine, and automotive [11–13]. A crucial aspect of the quality of obtained composites is the manufacturing quality, which significantly influences the uniform distribution of reinforcement material in the matrix [14, 15]. Composite materials, through their modification capabilities, have been employed as structural elements with open or closed cross-sections [16, 17]. Columns produced in this manner serve as load-bearing elements, which, due to their failure mechanism, are a more efficient and safer alternative to traditional columns made of conventional materials (steel or aluminum alloys). Numerous studies demonstrate a safe range between damage initiation and loss of load-carrying capacity in composite materials elements [18–20].

Failure analysis of these sandwich structures is crucial to understanding their mechanical behavior under various loading conditions. The distinctive properties of aluminum foam lead to complex failure mechanisms, including core crushing, shear failure, and delamination at the interface between the foam and composite layers. These failure modes can significantly impact the structural integrity and durability of the composite cladding, making it imperative to analyze the factors contributing to these failures. Recent studies have utilized advanced experimental techniques and computational methods to investigate these phenomena, providing insights into the stress distribution and damage evolution within the structure.

Giammaria's et al investigated the low-velocity impact behavior of flax, basalt, and hybrid bio-composite laminates across a temperature range (-40 °C to 80 °C), using experimental testing, analytical modeling, and numerical simulations [21]. Results showed that temperature significantly affected the response of flax composites, while basalt and hybrid materials demonstrated greater robustness. Analytical and numerical models provided reasonable predictions, highlighting the potential of these tools for design and optimization, though further refinements are needed to fully capture damage mechanisms at extreme temperatures.

Wei et al. [22] conducted research on the resistance of carbon fiber grid sandwich composite structures to high-velocity impact, which is of significant importance in the aerospace and automotive industries. The investigation encompassed experimental tests and computational simulations of various configurations of these structures to evaluate their strength and capacity for impact energy

absorption at high velocities. The findings demonstrated that an appropriate lattice structure, in conjunction with the properties of the carbon composite, substantially enhances damage resistance while maintaining low mass. These structures exhibit exceptional impact energy attenuation performance, rendering them promising materials for applications requiring high-speed impact resistance.

Sahib et al. present a comprehensive study on improving the performance of composite sandwich structures using advanced computational techniques [23]. The scope of the research includes the development and application of an artificial neural network (ANN) model to accurately predict the mechanical properties of these structures, which is critical for effective design optimization. Combined with a genetic algorithm (GA), the study aims to achieve multi-objective optimization that balances competing criteria such as weight reduction and strength enhancement. The results show significant performance improvements in the design of composite sandwich structures, presenting optimal configurations that outperform traditional designs in terms of performance metrics. These results highlight the potential for integrating artificial intelligence-based methods into materials engineering, providing a path for future innovations in structural design and optimization. The use of various neural network models has found application in many scientific fields as a tool for predicting indicators that determine mechanical or material properties [24–26].

The development of new technologies makes it possible to produce additive structures with porous composition. An interesting approach in the analysis of structures made using 3D technology was presented by Epasto et al. [27]. In this paper, the author presented a three-point bending analysis of sandwich structures printed from PLA polymer material. The structures in the bending plane had a honeycomb arrangement of different sizes, which translated into load carrying capacity. The results of this research highlight the significant potential of foam additive manufacturing (FAM) in the field of environmental sustainability.

Manufacturing samples by 3D printing from metal powders has numerous benefits, which were mentioned in the previous paragraph [28–30]. However, it is important to note the cons that this technology brings. The main disadvantages relate to the limitation in the printing of closed pores, which are important from a stress transfer point of view. Discontinuities in the form of open

pores can result in the occurrence of notches and stress concentrations that cause sudden cracking of the structure [31].

Aluminum foam castings produced by the liquid method, in addition to their many advantages, can have some significant disadvantages that affect the chosen mechanical properties [32, 33]. The main disadvantage is the formation of macro and micro pores when gases become trapped in the metal during casting, reducing the density and strength of the material. The non-uniformity of the pore distribution means that the casting can have variable mechanical properties at different locations, leading to a weakening of the strength of selected regions of the material [34, 35]. Another defect is cracks and deformations occurring due to internal stresses caused by uneven cooling of the metal, which can lead to weakening of the structure. The last major defect in cast foams are gas inclusions and inclusions, i.e. impurities that alter the microstructure of the casting, weakening its strength and corrosion resistance [36]. In addition, the rudimentary quality control resulting from the specific porous structure of aluminum foams makes it difficult to detect defects by traditional methods, requiring advanced non-destructive diagnostic techniques. Each of these defects affects the quality and durability of the castings, so their monitoring during the production process is extremely important to obtain a high-quality structure.

Furthermore, improving the design of aluminum foam and composite sandwich panels requires a thorough understanding of how different parameters, such as core density, composite type, and loading rate, influence their failure behavior. As the demand for lightweight and

high-performance materials continues to rise, addressing these challenges through detailed failure analysis will pave the way for the development of more resilient and efficient sandwich structures.

Theoretical background

Aluminum as well as fiber reinforced polymer are two materials distinguished by their mechanical properties and behaviors under stress, making them suitable for diverse engineering applications. Aluminum, a lightweight metal, exhibits considerable malleability and enables both elastic and plastic deformation (Fig. 1) when subjected to external loads [37]. This characteristic allows aluminum to endure certain degrees of bending and deformation prior to failure. However, once the material surpasses its yield strength, it can undergo permanent deformation, ultimately leading to mechanical failure through mechanisms such as cracking or fracture, particularly in regions of stress concentration, including joints and notched configurations. Consequently, aluminum’s relatively predictable failure modes make it a common choice in applications where ductility and malleability are advantageous [38, 39].

In contrast, a fiber composite material that integrates high-performance fibers with a resin matrix, resulting in a material that offers superior strength-to-weight ratios and rigidity compared to traditional metals. CFRP typically displays limited plastic deformation, indicating that while it demonstrates significant resistance to bending, it is also prone to sudden and catastrophic failure under excessive loads (Fig. 1). The failure mechanisms associated with CFRP include

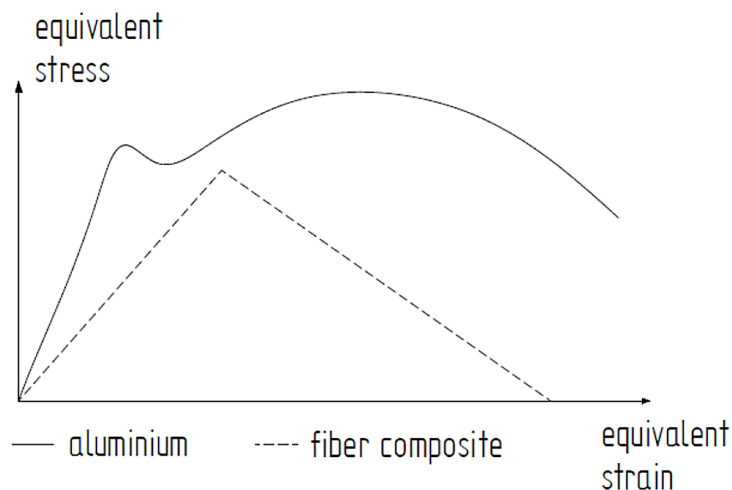


Figure 1. Exemplary stress – strain curve for aluminum and fiber composite

fiber pull-out, matrix cracking, and delamination, which can render the material's failure modes less predictable than those of aluminum. Therefore, the selection between aluminum and CFRP necessitates careful consideration of the specific requirements of the application, including weight constraints, desired mechanical properties, and anticipated loading conditions. This understanding is essential for optimizing material performance in engineering designs.

The plastic deformation of metallic foams deviates significantly from that of monolithic materials due to their inherently porous microstructure. Deformation mechanisms encompass cell wall bending (dominant in open-cell foams under low hydrostatic stress), cell wall stretching (more prominent under higher hydrostatic pressures), ligament shear and fracture (often initiating failure), and complex node deformation [40–42]. The resulting yield behavior is highly sensitive to hydrostatic pressure and deviatoric stress components, deviating from simple yield criteria such as von Mises, and exhibiting substantial stress-path dependence [43].

Yield surfaces are often non-standard shapes (e.g., elliptical or quadratic), reflecting the complex interaction of deformation mechanisms. Strain hardening is typically accompanied by densification, as cells collapse and ligaments fracture, ultimately leading to failure. Accurate constitutive modeling requires consideration of these coupled phenomena, necessitating sophisticated models that capture the interplay of microstructure, loading conditions, and evolving material properties throughout plastic deformation.

MATERIALS AND METHODS

In this research, the development and manufacture of sandwich structures utilizing an aluminum foam core reinforced with various cladding

materials to enhance mechanical properties was focused on. The core was constructed from aluminum foam, known for its lightweight and excellent energy absorption characteristics. The cladding consisted of an aluminum sheet, a carbon fiber-reinforced polymer sheet, and a flax fiber-reinforced polymer sheet, chosen for their superior strength-to-weight ratios and sustainability (Fig. 2). Each specimen was carefully manufactured with dimensions of $140 \times 40 \times 20$ mm through a meticulous adhesive process that bonded the cladding layers to the aluminum foam core. This methodical assembly aimed to evaluate the mechanical performance and potential applications of these innovative composite structures in various engineering fields.

The metal foam used in this study was manufactured in-house at the foundry laboratory of the Maritime University of Technology in Szczecin. The porous structure obtained is characterized by closed pores with a regular shape. The foam was formed by applying the foaming-in-liquid method described in detail in the authors' previous publications [44]. The fundamental process involved the liquefaction of the aluminum alloy AlSi9, followed by the incorporation of calcium to enhance the viscosity of the liquid alloy. The aluminum alloy was heated above its liquidus temperature, after which TiH_2 powder was introduced as a foaming agent. Due to the elevated temperature, titanium hydride decomposed into titanium metal and hydrogen gas. The resultant foam was cooled below the solidus temperature to stabilize the structure. The porous structure formed upon cooling was subsequently cut to the desired dimensions. The adhesive bonding of the sandwich structures was also performed in-house and the subsequent steps are shown in Figure 3.

To determine the properties of the self-generated metal foam, gas adsorption tests were carried out using the Brunauer-Emmett-Teller (BET) method (Table 1). The test determines the quality

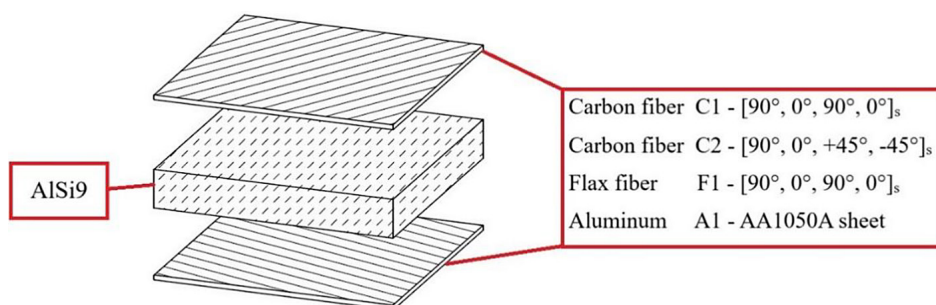


Figure 2. Schematic presentation of research materials

of the generated porous structure by determining its density and the percentage of closed and open pores. The analysis was performed using N_2 gas at 20.3 °C, the target pressure was 5.0 psig. The analysis was carried out for four samples with volumes in the range 3.68–3.70 cm^3 .

Aluminum foam and the composite panels supplied by the manufacturer were used to create a sandwich structure by bonding the cladding to both sides of the metal foam (core). The formation of a permanent bond was accomplished by using Epidian 53 epoxy resin and Z1 polyamide hardener at a ratio of 10:1. The resulting adhesive bond is characterized by high flexibility and impact resistance, which is crucial for the planned scope of the study. Bonding took place according to the guidelines presented in the literature as well as the adhesive manufacturer’s instructions. In a first step, the bonded surfaces were degreased and then a layer of adhesive mixture was applied to the top layer of the cladding. The previously prepared metal foam (core) was then applied to the upper surface. The core was then loaded for 8–12 hours until the cladding-core bond was cured. The operation was

then repeated with the second cladding, creating an interlayer structure consisting of a lightweight core with composite facings. The prepared specimens were left to fully cure for 7–10 days before bench testing at room temperature.

Experimental tests were carried out on an MTS 793 universal testing machine with a sensor built into the head with a test range of 0–50 kN. A 140 × 40 × 20 mm specimen was placed on 5 mm radius supports spaced 100 mm apart (Figure 4). The upper crosshead placed centrally moved vertically 2 mm/min. The experimental test was realized on the basis of the standard ASTM C393 [45].

The experimental specimens had a core thickness of about 18 mm and cladding made of different structural materials (Table 2). Two samples had CFRP cladding with fiber orientation $[90^\circ, 0^\circ, 90^\circ, 0^\circ]_s$ designated as C1 in the results. Two more samples had an arrangement $[90^\circ, 0^\circ, +45^\circ, -45^\circ]_s$ designated as C2 in the results. Epoxy resin-reinforced flax fiber specimens had an arrangement $[90^\circ, 0^\circ, 90^\circ, 0^\circ]_s$ designated as F1 in the results. For all composite panel sandwich specimens, the cladding was placed

Table 1. Results of gas adsorption analysis

Name	Value	Standard deviation
Average volume [cm^3]	3.6981	0.0037 cm^3
Average density [g/cm^3]	1.0313	0.0010 cm^3
Average open cell [%]	76.3322	0.0236%
Average closed cell [%]	23.6681	0.0236%

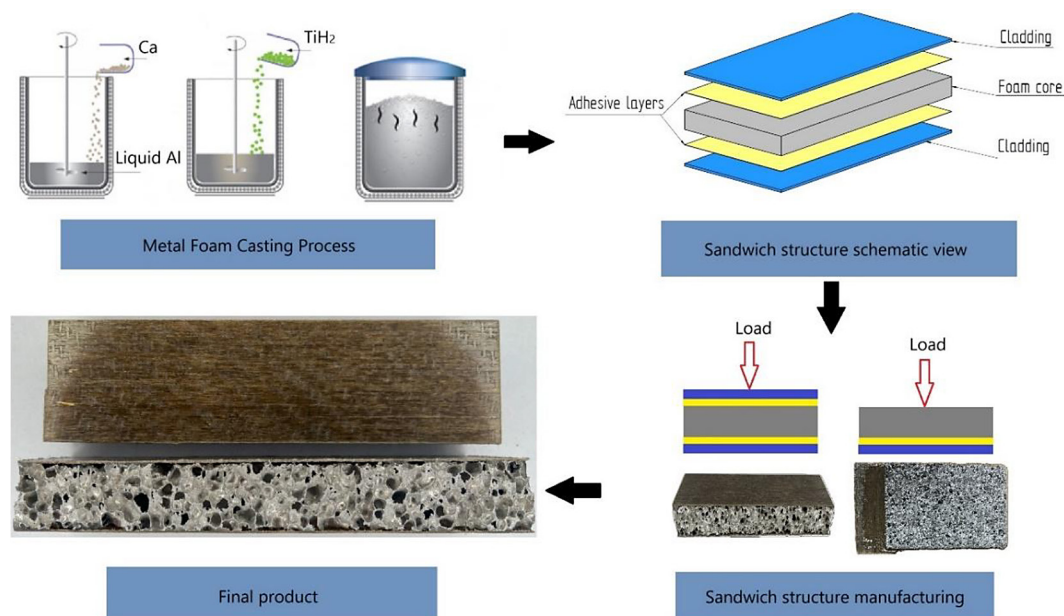


Figure 3. Manufacturing process of metal foam sandwich structure

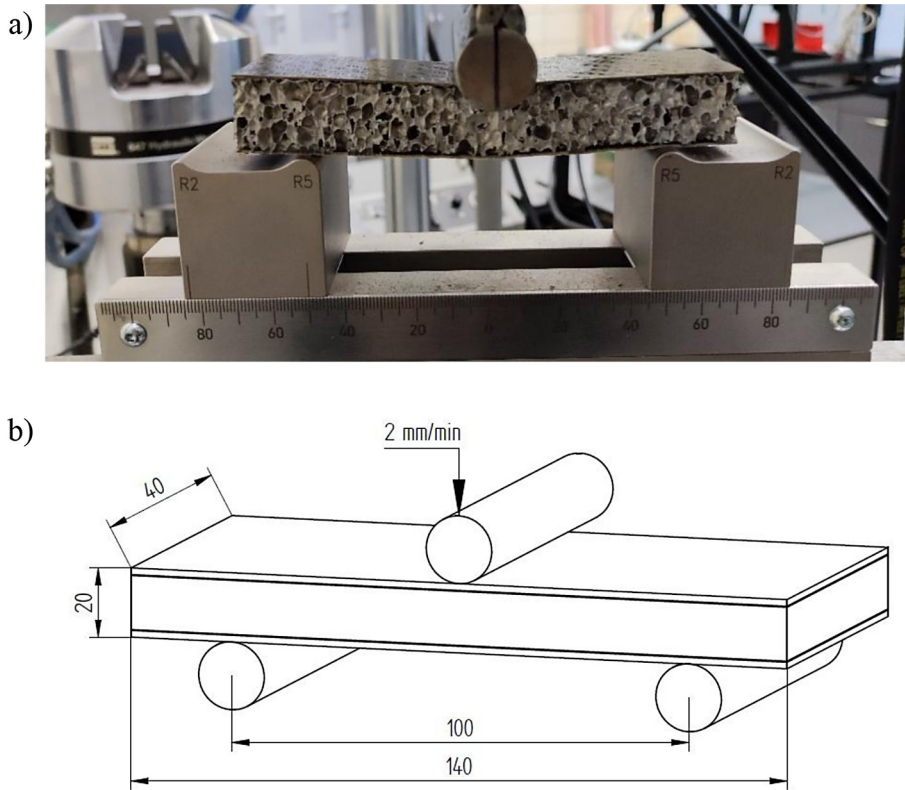


Figure 4. Testing stand condition (a) actual view (b) schematic view

Table 2. Comparison of research test condition for different specimen

Name	Cladding material	Core material	Crosshead velocity [mm/min]	Stacking sequence
C1	Carbon fiber	AlSi9	2	[90°, 0°, 90°, 0°]
C2	Carbon fiber			[90°, 0°, +45°, -45°]
F1	Flax fiber			[90°, 0°, 90°, 0°]
A1	Aluminum sheet			N/A

symmetrically with respect to the foam core. In addition, two samples with AA1050A aluminum sheet cladding, designated A1 in the publications, were tested.

In addition, in order to observe and accurately present the damage to the porous core as well as the composite cladding, a Keyence VHX 970F digital microscope was used for analysis. The microscope is equipped with a movable head that allows recording images at any tilt angle. The present study was carried out at an approximation of x20, which, for all samples, allowed accurate observation of the degradation of the sandwich structure.

RESULTS

The bench tests were carried out with constant boundary conditions for all specimens with

the same dimensions. The specimens differed in the type of cladding used, which affects the load transfer and degradation behavior of the composite sandwich structures. Bench tests carried out for a displacement of the upper crosshead of 20 mm in the vertical direction. Larger crosshead displacement resulted in wedging of the wrapped sandwich structure. The sampling frequency was set as 20 Hz, which allowed obtaining around 12,000 measurement points. Such a large number of points is necessary in order to correctly determine the location of a structural failure characterized by a sudden drop in force value.

All the results presented revealed a higher hardening rate characterized by the plateau region after the point of yielding associated with the plastic deformation of the structure. The shape of the curve then deviates from those presented in

the work of Zhang et al. as a reference for three-point bending of sandwich structures [46].

In the analysis of the test results, several factors important for the three-point bending test were taken into consideration. The first aspect analyzed is the extent of elastic deformation of the structure, which can be observed in the first stage of force increase in the force-displacement diagrams in Figures 5–12. The slope of the curve in the first stage of bending showed a higher Young’s modulus for the two types of cladding materials A1 and C2. Specimens C1 and F1 showed a slightly lower modulus resulting in a 2 mm deformation of the structure in the elastic range. The curve for sample A1 shows a high convergence for both specimens (Fig. 5).

In order to simply identify the deformation of the structure with respect to the change in force as a function of displacement, a graphical representation of the post-crush spacer structures was placed next to the curves. This methodology was applied to all presented specimens. Static

three-point bending test of A1 specimens showed high compliance of a critical force of about 1200 N, as well as further deformation of the structure. The test specimen with aluminum sheet cladding (A1), after obtaining the critical force, obtained a constant value called the “plateau” region. The specific course of the function of the force value, indicates significant energy absorption properties confirmed occurrence of a progressive course of force values for selected samples.

The next analyzed samples had a C1 designation and cladding made of carbon fiber reinforcement polymer. The fiber arrangement is symmetrical with respect to the porous core. The analysis conducted showed a slight discrepancy in the value of the critical force. The shape of the curve is similar for the two samples tested, while sample S1 is characterized by slightly lower force values resulting from the indentation of the cladding into the aluminum foam.

The force diagram for specimen S1 has a visible drop in force around the 15 mm crosshead

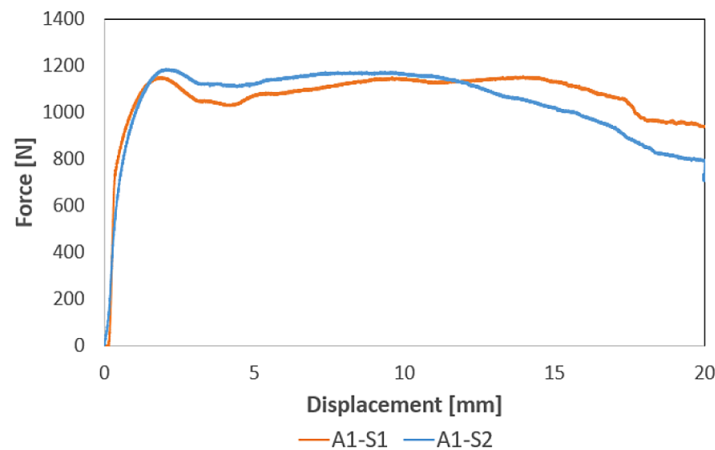


Figure 5. Force-displacement curve for A1 specimen

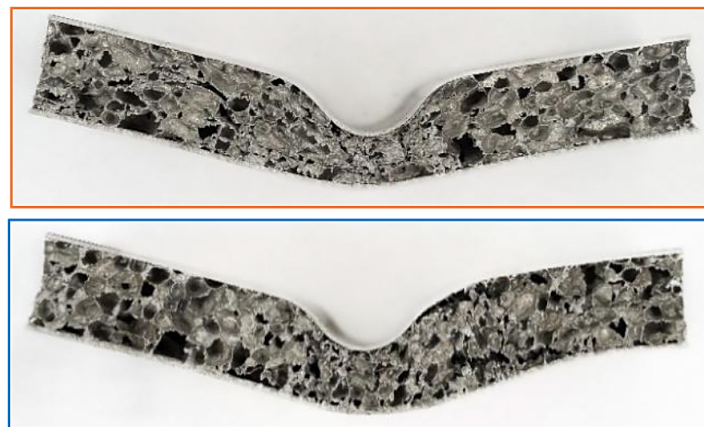


Figure 6. Frontal view of tested A1 specimen

displacement. This drop is related to the detachment of the cladding from the foam core visible in the top image in Figure 8. The post-bending specimens have a visible uniform distribution of pores, which did not crush beyond the central part of the specimen. As a result of the bending of both specimens, fiber cracking of the upper cladding occurred, which is visible in Figure 7 as spikes in force values. The failure analysis of the sandwich structure is described in more detail later in the results.

Another specimen labelled C2 showed a constant crushing force in terms of plastic deformation of the structure. Specimen C2 had +/- 45° fibers, which reinforce the structure during flexural deformation of the cladding in both fiber tension and compression. Similarly to specimen C1, specimen S1 has a marked decrease in force

values due to cladding detachment (Fig. 9–10). The failure of the structure is caused by significant shear stresses. Despite the damage to the adhesive bond, the structure is capable of carrying the load. The force values recorded from 10 mm of head displacement indicate higher force values for the specimen with detached cladding. From the diagram (Fig. 9), it can be concluded that the use of thin cladding allows the sandwich structure to effectively absorb mechanical energy even after structural failure has occurred.

The last type of specimen analyzed had cladding made of flax fibers in an epoxy resin matrix. The deformation of the structure followed a similar pattern throughout the three-point bending stage. Despite the visual similarity of specimens S1 and S2 (Fig. 12), differences in the force-shortening curves are apparent (Fig. 11). Furthermore,

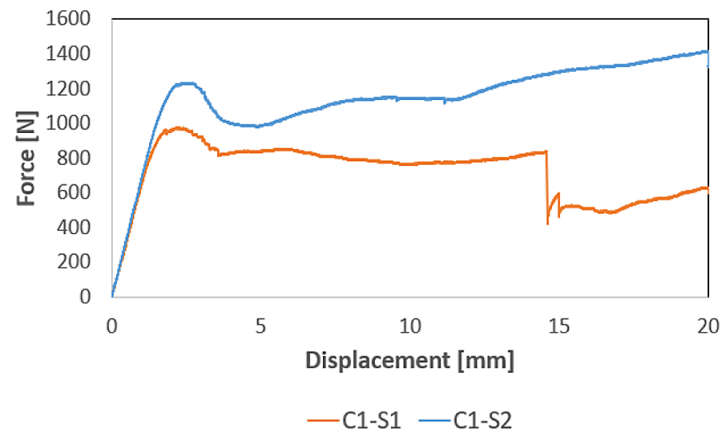


Figure 7. Force-displacement curve for C1 specimen

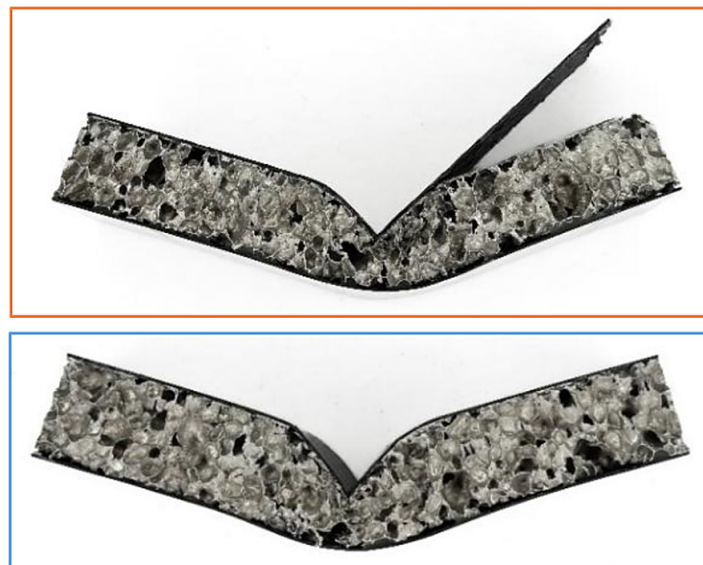


Figure 8. Frontal view of tested C1 specimen

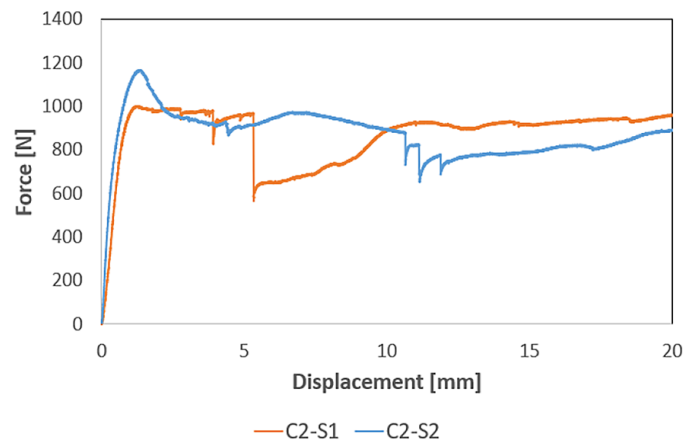


Figure 9. Force-displacement curve for C2 specimen



Figure 10. Frontal view of tested C2 specimen

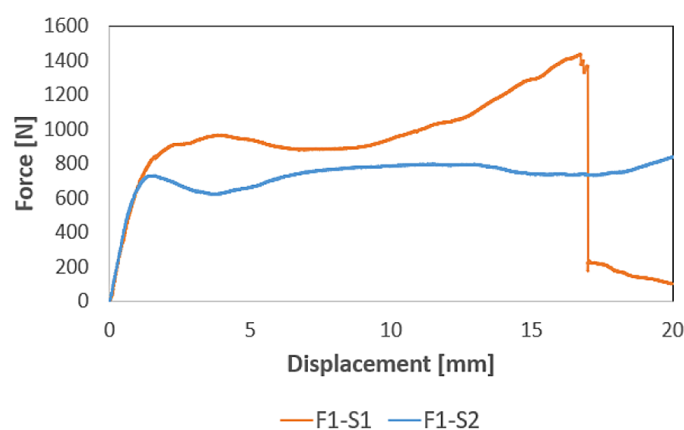


Figure 11. Force-displacement curve for F1 specimen

in the region of 17 mm, a sharp drop in force values associated with complete fracture of the lower lining is evident. As the linen composite has a significantly lower tensile strength than the

carbon composite, a different failure mode of the sandwich structures was observed. Observing the recorded force values for all samples, it is worth noting that the F1 model with flax fiber showed a



Figure 12. Force-displacement curve for F1 specimen

progressive course for both specimens. The difference in the height of the curves may be due to the pore distribution in the aluminum foam.

Based on all the results presented above, two characteristic values were determined for flexural specimens with different cladding materials. The values determined refer to the critical force, i.e. the value of the force recorded at the transition from elastic to plastic deformation. The force values are summarized in Table 3, allowing the force values relating to the energy absorbed by models with specific parameters. The critical force varies from 969 to 1232 N, which is due to the type of cladding used. The highest values of both force and energy absorbed were obtained for sample C1-S2. The significant variations in the values shown in Table 3 are due to the nature of the plastic deformation and structural failure as should be observed in the force-displacement curves above.

In a three-point bending test, structures with metal foam and adhesive fiber composite cladding can be damaged by several types of failure. Fiber composites can fail by matrix cracking, separation of fibers from the matrix, fiber cracking, crushing under compressive forces, as well as delamination, which is the separation of composite layers. During the test, when the load is applied at the center point, local deformation of the metal foam core can occur, leading to crushing or cracking. In addition, in the case of an

adhesive joint, bending of the specimen can cause the detachment of the composite cladding from the core, leading to a loss of structural integrity and a significant weakening of the load-bearing capacity of the structure most often caused by significant shear stresses. All this damage leads to a weakening of the mechanical properties of the hybrid sandwich structure, reducing its strength and stiffness. Despite the occurrence of significant damage to the structure, the study showed that the application of appropriate cladding allows the structure to continue to carry loads. The following figures illustrate in detail the types of damage that occurred during the bench tests. The first type of damage involving metal foam cracking, shown in Figure 13, refers to specimen A1. The metal foam under three-point bending undergoes shear cracking between the cladding layers.

The next two photos present cladding failure made of carbon-fiber reinforced polymer. Figures 14 and 15 show the break line occurring at the pressure point of the upper crosshead. The shape of the line differs for specimen C1 and C2, which is due to the additional reinforcement of the $\pm 45^\circ$ layer. In Figure 15, the breakthrough line of the top layer is skewed, which is visible in both the top photo and the close-up of the damage. In addition, comparing the damage figure of the structure with the force-displacement diagram, a gradual cracking of the composite layer is

Table 3. Critical force value all tested specimen

Specimen	A1-S1	A1-S2	C1-S1	C1-S2	C2-S1	C2-S2	F1-S1	F1-S2
P_{cr} [N]	1152.8	1187.6	977.4	1232.6	1002.8	1167.7	969.0	1087.6

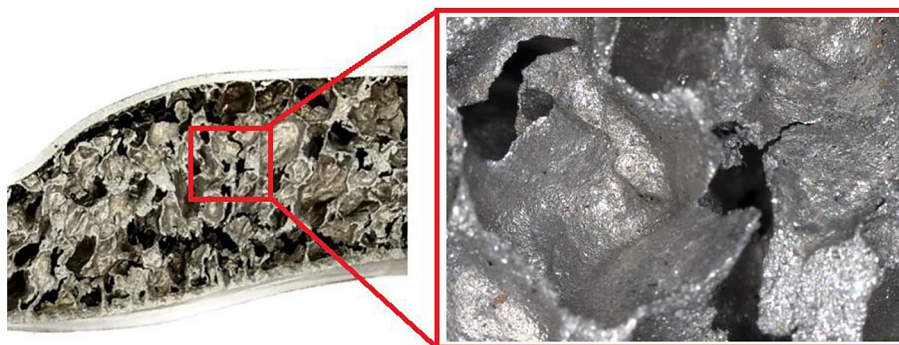


Figure 13. Foam fracture presentation based on A1 specimen (zoom x20)

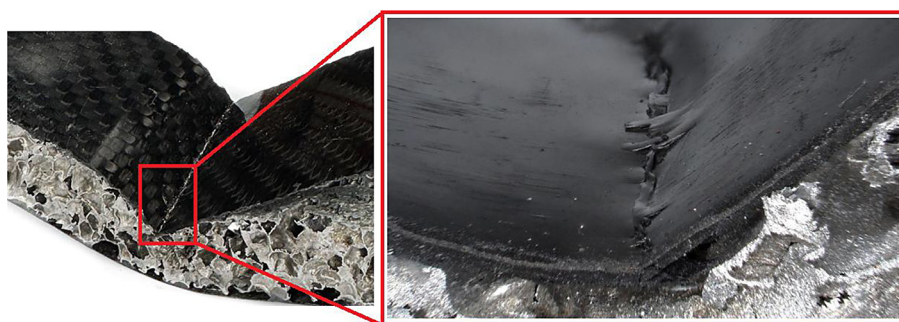


Figure 14. Matrix cracking on the fracture line for C1 specimen (zoom x20)



Figure 15. Fracture line for CFPR cladding based on C2 specimen (zoom x20)

noticeable, visible as gradual drops in force values at different moments of displacement. Based on the results, it can then be concluded that during deformation the load-carrying capacity is due to the foam core applied. The cladding used and the orientation of its fibers intensify the performance of the sandwich structure improving its ability to carry loads in the complex state.

The last type of samples analyzed (F1) is a sandwich construction of metal foam and flax composite cladding. Natural fibers in a polymer resin matrix became popular through their high availability and low price. On the other hand, natural fibers have a heterogeneous structure by

which they must be carefully controlled during the flax pad manufacturing process. On the basis of the realized research, it was found that the fibers have the ability to carry relatively high loads, while undergoing rapid damage associated with fiber cracking. The breakage line seen in Figure 16 for sample F1-S1 occurred when the crosshead displaced by 17 mm. This damage resulted in a complete loss of load carrying capacity visible in the force-displacement diagram (Figure 11), a significant drop in force from 1400 N to 200 N.

In the case of the last graphic for sample F1-S2, the detachment of the cladding in the area of the upper crosshead is visible. As a result of the



Figure 16. Total damage of the lower flax cladding for the F1-S1 specimen (zoom x20)

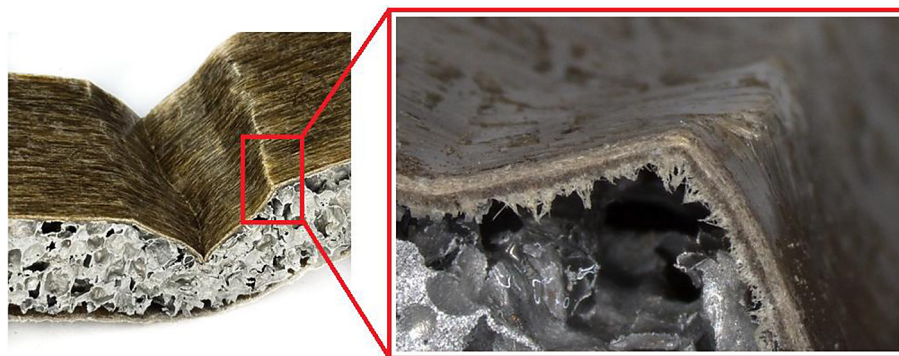


Figure 17. Fiber crack based on F1-S2 specimen (zoom x20)

stuck upper roll, there was fiber damage visible in the close-up (Fig. 17). Cladding cracking occurred from the front edge of the model and progressed toward the rear edge of the sample. In fact, the different types of cladding used translate into load-carrying capacity, as shown in the results in the charts and the graphical failure of the materials. The material that mainly accounts for the load-bearing capacity of the structure is metal foam, whose deformation and failure mode has large plateau ranges during compression, which translates into a high capacity to absorb mechanical energy. In addition, the porous structure ensures stress distribution regardless of the direction of stress, making the structure highly isotropic.

CONCLUSIONS

The presented research results concerned the experimental analysis of three-point bending of hybrid sandwich structures. The study analyzed the effect of the application of different types of cladding on the load-carrying capacity, as well as the structural degradation analysis of both the core

and cladding. The tests were carried out on a universal testing machine. Analyses were conducted with a fixed support arrangement for a displacement of the upper crosshead of 2 mm/min up to 20 mm. This value for all types of specimens showed significant plastic deformation of the structure and accompanying failure of the core and cladding. Based on microscopic analysis, it was revealed that during three-point bending it is possible to observe pore cracking of the metal foam, detachment of the cladding or fiber cracking of the composite material. The influence of materials with different deformation character on the application possibilities in sandwich structures with metal foam was analyzed. Based on the study, it was found:

- the load-carrying capacity strongly depends on the porous core applied,
- the cladding material affects the way the sandwich structure deforms, in addition different cladding caused an increase in critical force of sandwich structure by nearly 26% comparing samples C1 and F1,
- in the case of high stiffness cladding (CFRP), there is a risk of cladding debonding caused by high shear stresses,

- despite the occurrence of cladding debonding at the early stage of bending (C2-S1), the subsequent stage of bending reveals a high capacity for further absorption of mechanical energy even higher than for sample C2-S2 whose crushing proceeded with no prior detachment,
- linen composite, despite its lower strength than carbon composite, has similar load-carrying capacity,
- the quality of the cast foam, the distribution of pores their quality and shape greatly affects the ability to carry loads.

Acknowledgement

The research leading to these results has received funding from the commissioned task entitled “VIA CARPATIA Universities of Technology Network named after the President of the Republic of Poland Lech Kaczyński” under the special purpose grant from the Minister of Education and Science, contract no. MEiN/2022/DPI/2575, as part of the action “In the neighborhood - inter-university research internships and study visits.”

REFERENCES

1. Rogala M, Gajewski J. Crashworthiness analysis of thin-walled square columns with a hole trigger. *Materials (Basel)*. 2023; 16: 4196.
2. Xiang J, Du J. Energy absorption characteristics of bio-inspired honeycomb structure under axial impact loading. *Mater. Sci. Eng. A* 2017; 696: 283–9.
3. Rogala M, Tuchowski W, Czarnecka-Komorowska D, Gawdzińska K. Analysis and assessment of aluminum and aluminum-ceramic foams structure. *Adv. Sci. Technol. Res. J.* 2022; 16: 287–97.
4. Vesenjak M, Duarte I, Baumeister J, Göhler H, Krstulović-Opara L, Ren Z. Bending performance evaluation of aluminium alloy tubes filled with different cellular metal cores. *Compos. Struct.* 2020; 234.
5. Kulshreshtha A, Dhakad SK. Preparation of metal foam by different methods: A review. *Mater. Today Proc.* 2020.
6. Ha NS, Lu G. A review of recent research on bio-inspired structures and materials for energy absorption applications. *Compos. Part B Eng.* 2020; 181.
7. Sun J, Fang H. The analysis of crashworthiness and dissipation mechanism of novel floating composite honeycomb structure against ship-OWT collision. *Ocean Eng.* 2023; 287: 115819.
8. Gawryluk J. The effect of fiber arrangement in the bio-laminate and geometric parameters on the stability of thin-walled angle column under axial compression. *Adv. Sci. Technol. Res. J.* 2023; 17: 150–9.
9. Nicolinco C, Mahboob Z, Chemisky Y, Meraghni F, Oguamanam D, Bougherara H. Prediction of the compressive damage response of flax-reinforced laminates using a mesoscale framework. *Compos. Part A Appl. Sci. Manuf.* 2021; 140: 106153.
10. Xing J, Zhao J, Niu Q, Zhang T, Zhang C, Zhang Y, et al. Crashworthiness design and optimization of bamboo-inspired tube with gradient multi-cells. *Thin-Walled Struct.* 2023; 191: 111034.
11. Rozylo P. Failure phenomenon of compressed thin-walled composite columns with top-hat cross-section for three laminate lay-ups. *Compos. Struct.* 2023; 304: 116381.
12. Wang Z, Jin X, Li Q, Sun G. On crashworthiness design of hybrid metal-composite structures. *Int. J. Mech. Sci.* 2020.
13. Qvale K, Hopperstad OS, Morin D, Børvik T. Micro-mechanics-based simulation of quasi-static and dynamic crushing of double-chamber 6000-series aluminium profiles. *Int. J. Impact Eng.* 2023; 180: 104636.
14. Różyło P, Smagowski W, Paśnik J. Experimental research in the aspect of determining the mechanical and strength properties of the composite material made of carbon-epoxy composite. *Adv. Sci. Technol. Res. J.* 2023; 17: 232–46.
15. Rozylo P, Rogala M, Pasnik J. Buckling analysis of thin-walled composite structures with rectangular cross-sections under compressive load. *Materials (Basel)*. 2023; 16.
16. Debski H, Rozylo P, Wyszumski P, Falkowicz K, Ferdynus M. Experimental study on the effect of eccentric compressive load on the stability and load-carrying capacity of thin-walled composite profiles. *Compos. Part B Eng.* 2021; 226: 109346.
17. Debski H, Samborski S, Rozylo P, Wyszumski P. Stability and load-carrying capacity of thin-walled FRP composite z-profiles under eccentric compression. *Materials (Basel)*. 2020; 13: 2956.
18. Rozylo P, Rogala M, Pasnik J. Load-carrying capacity of thin-walled composite columns with rectangular cross-section under axial compression. *Materials (Basel)*. 2024; 17: 1615.
19. Śledziwski K, Górecki M, Gajewski J, Rogala M. Parametric Study of Girders with Sinusoidal Corrugated Web. *Materials (Basel)*. 2024; 17: 6079.
20. Rozylo P. Limit states of thin-walled composite structures with closed sections under axial compression. *Compos. Part B Eng.* 2024; 287: 111813.
21. Giammaria V, Boria S, Sarasini F, Tirillò J, Cognigni F, Rossi M, et al. Low-velocity impact behaviour of biocomposite laminates reinforced by flax, basalt and hybrid fibres at various temperatures:

- Analytical, numerical and experimental results. *Compos. Struct.* 2023; 322: 117332.
22. Wei S, Guo Z, Niu W, Chai GB, Tai Z, Li Y. High-velocity impact resistance of the carbon fiber composite grid sandwich structures. *Polym. Compos.* 2024; 45: 5558–73.
 23. Mohammed Sahib M, Kovács G. Multi-objective optimization of composite sandwich structures using Artificial Neural Networks and Genetic Algorithm. *Results Eng.* 2024; 21: 101937.
 24. Gajewski J, Rogala M, Vališ D. Application of neural networks specific forms for estimation of crushing signal parameters of multilevel structural absorbers implemented in passive safety research. *Measurement* 2025; 242: 115817.
 25. Ferdynus M, Gajewski J. Identification of crashworthiness indicators of column energy absorbers with triggers in the form of cylindrical embossing on the lateral edges using artificial neural networks. *Eksploat. i Niezawodn.* 2022; 24: 805–21.
 26. Vališ D, Hasilová K, Gajewski J, Rogala M. Proper functioning and failure occurrence of energy absorbers modelled for optimization. *Eng. Fail. Anal.* 2025; 170: 109238.
 27. Epasto G, Rizzo D, Landolfi L, Detry ALHS, Papa I, Squillace A. Design of monomaterial sandwich structures made with foam additive manufacturing. *J. Manuf. Process.* 2024; 121: 323–32.
 28. Sonti KSM, Penumakala PK, Narala SKR, Vincent S. Experimental and numerical analysis of the compression behavior of aluminum syntactic foams reinforced with alumina hollow particles. *Eng. Struct.* 2024; 300: 117144.
 29. Viscusi A, Carrino L, Durante M, Formisano A. On the bending behaviour and the failure mechanisms of grid-reinforced aluminium foam cylinders by using an experimental/numerical approach. *Int. J. Adv. Manuf. Technol.* 2020; 106: 1683–93.
 30. Doroszko M, Seweryn A. Numerical modelling of the mesofracture process of sintered 316L steel under tension using microtomography. *Eng. Fract. Mech.* 2021; 255.
 31. Doodi R, Gunji BM. Prediction and experimental validation approach to improve performance of novel hybrid bio-inspired 3D printed lattice structures using artificial neural networks. *Sci. Rep.* 2023; 13: 1–17.
 32. Zhang X, Cai ZY, Gao JX, Liang XB. Face sheet defects in plastic forming of aluminum foam sandwich panel: theoretical models, numerical and experimental studies. *J. Mater. Res. Technol.* 2023; 26: 4351–64.
 33. Yuan K, Xia Z, Wang L, Wu L. Mechanical properties and failure analysis of ring-stiffened composite hulls under hydrostatic pressure. *Compos. Struct.* 2025; 351: 118609.
 34. Zhang X, Chen QM, Cai ZY. Prediction and prevention of fracture defect in plastic forming for aluminum foam sandwich panel. *J. Mater. Res. Technol.* 2021; 15: 1145–54.
 35. Bejger A, Gawdzińska K. Identification of structural defects of metal composite castings with the use of elastic waves. *Arch. Metall. Mater.* 2011; 56.
 36. Kádár C, Kubelka P, Szlancsik A. On the compressive properties of aluminum and magnesium syntactic foams: Experiment and simulation. *Mater. Today Commun.* 2023; 35.
 37. Xu J, Hopperstad OS, Holmedal B, Berstad T, Mánik T, Marthinsen K. On the spatio-temporal characteristics of the Portevin-Le Chatelier effect in aluminium alloy AA5182: An experimental and numerical study. *Int. J. Plast.* 2023; 169.
 38. Balkrishna Tandale S, Markert B, Stoffel M. Intelligent stiffness computation for plate and beam structures by neural network enhanced finite element analysis. *Int. J. Numer. Methods Eng.* 2022; 123: 4001–31.
 39. Homayounfard M, Ganjiani M. A large deformation constitutive model for plastic strain-induced phase transformation of stainless steels at cryogenic temperatures. *Int. J. Plast.* 2022; 156: 103344.
 40. Cao M, Qiu T, Deng B, An Y, Xing Y, Zhao E. Materials & Design Construction and deformation behavior of metal foam based on a 3D-Voronoi model with real pore structure. *Mater. Des.* 2024; 238: 112729.
 41. Simone AE, Gibson LJ. Aluminum foams produced by liquid-state processes. *Acta Mater.* 1998; 46: 3109–23.
 42. Lakes RS. Cellular solids. *J. Biomech.* 1989; 22: 397.
 43. Deshpande VS, Fleck NA. Isotropic constitutive models for metallic foams. *J. Mech. Phys. Solids* 2000; 48: 1253–83.
 44. Rogala M, Ferdynus M, Gawdzińska K, Kochmański P. The influence of different length aluminum foam filling on mechanical behavior of a square thin-walled column. *Materials (Basel)*. 2021; 14: 3630.
 45. ASTM International. Standard test method for core shear properties of sandwich constructions by beam flexure (ASTM C393/C393M-20). *ASTM Int.* 2020; i: 1–7.
 46. Zhang Z, Zhang Z, Liu N, Xia X, Wang Z, Wang J, et al. Three-point bending performances of integral-forming aluminum foam sandwich. *Mater. Des.* 2023; 229: 111889.